THIRD EUROPEAN ROTORCRAFT AND POWERED LIFT AIRCRAFT FORUM

Paper No. 23

ACTIVE HELICOPTER ROTOR-ISOLATION WITH APPLICATION OF MULTI-VARIABLE FEEDBACK CONTROL

H. Strehlow, R. Mehlhose, M. Obermayer

Messerschmitt-Bölkow-Blohm GmbH
Munich, Germany

September 7 - 9, 1977

Aix-en-Provence, France

ASSOCIATION AERONAUTIQUE ET ASTRONAUTIQUE DE FRANCE

ACTIVE HELICOPTER ROTOR-ISOLATION WITH APPLICATION OF MULTI-VARIABLE FEEDBACK CONTROL [1)]

H. Strehlow, R. Mehlhose, M. Obermayer
Messerschmitt-Bölkow-Blohm GmbH
Munich, Germany

Summary

In the past different methods for reducing rotor-induced fuselage vibration have been investigated. Very little attèntion has been given to active devices however, not only because of their complexity and cost, but, more importantly, because the theory had not been adequately developed. Modern control theory for multi-variable feedback design with disturbance rejection is a powerful tool for designing and developing an active rotor isolation system. This system takes care of the two following problems, (1) full rejection of unmeasurable harmonic rotor excitation and (2) elimination of relative motion of the gearbox during static or maneuver loads by means of a trim device. This paper discusses the theoretical investigations of an active nodal isolation system, which is now being developed in a research program for testing a laboratory research model. Disturbance rejection controllers have been designed both by Optimal Control and by the Second Method of Liapunov. The latter concept is able to tolerate structure flexibility even in the case of simple output feedback. The numerical results demonstrate that multi-axis, multi-frequency active rotor isolation is superior to any existing passive rotor isolation device. It is an attractive solution to the helicopter vibration problem, and, because of the advanced technology in hydraulic servo system and digital control by microprocessors, can be made practical in the near future.

Notation

A	actuator area
d, k	damper, spring
G	transfer function
K, k	coefficients
m	mass
N	number of rotor blades
p	pressure

[1)] Work sponsored by the German Ministry of Research and Technology (BMFT)

s	Laplace variable
t	time variable
TR	force transmissibility
V	Liapunov function
z	vertical deflection
ζ	damping ratio
$\psi = \Omega t$	rotor azimuth angle
Ω	rotor rotational frequency
ω	frequency
$\underline{a}$	acceleration
$\underline{A}$, $\underline{B}$, $\underline{W}$	plant matrices
$\underline{C}$, $\underline{D}$, $\underline{V}$	output matrices
$\underline{D}$, $\underline{K}$, $\underline{M}$	generalized damping-, stiffness- and mass matrices
$\underline{d}$	disturbance
$\underline{M}_\nu$	"notch mass"
$\underline{F}$	force
$\underline{K}$, $\underline{L}$	feedback matrices
$\underline{n}$	notch vector
$\underline{Q}$, $\underline{H}$	weighting matrices
$\underline{q}$	vector of the generalized coordinates
$\underline{r}$	reference signal
$\underline{u}$	control input
$\underline{x}$	state vector
$\underline{y}$	output vector
$\underline{\alpha}$, $\underline{\beta}$	weighting matrices
$\underline{\delta}$	relative isolator deflection
$\underline{T}$	transformation matrix

Subscripts

F	fuselage
I	isolator
R	rotor/transmission unit
L	Liapunov
m	measured
p	plant

Superscripts

$\dot{} = \frac{d}{dt} \equiv D$	time - differentiation
$' = \frac{d}{d\psi}$	azimuth angle - differentiation

1. Introduction

In translational flight helicopters are exposed to oscillatory hub loads mainly generated by the vibrations of the rotor blade aerodynamics during each rotor revolution.

These deterministic disturbances are harmonic with N/rev, 2N/rev etc. frequency components, where N is the number of rotor blades. Figure 1 shows two characteristic amplitude spectra of the vertical cabin vibrations of the helicopter BO 105 (4-blade-rotor) measured in transition and cruise speed flight.

New stringent requirements for crew and passengers comfort and for improved reliability and maintainability have forced the rotorcraft manufacturers to reduce the high vibration level of today's helicopters. There are different basic technical approaches to attenuate rotor-induced fuselage oscillations:

- Improved aerodynamic rotor design
- Structural dynamic tuning of the rotor blades
- Rotating system dynamic absorbers
- Structural dynamic tuning of the fuselage
- Nonrotating system dynamic absorbers
- Rotor isolation (isolating the fuselage from the rotor/transmission unit)
- Higher harmonic cyclic control of the rotor blade or of auxiliary lifting surfaces (flaps)

During the last twenty years extensive research and development work has been done in all areas with changing success, see for example References 1, 2 and 3.

Recent trends in helicopter vibration control seem to indicate that the industry has accepted the rotor isolation concept as the solution of the helicopter vibration problem.

In the past the majority of rotor isolation systems have employed more or less sophisticated transmission suspension elements which do not require a continuous power supply for operation. While for many applications the performance of passive rotor isolation systems (References 4 through 12) may be adequate, these systems are showing fundamental limitations compared with active vibration control. As pointed out in Reference 12 an active rotor isolation system can generally be designed to have the same effect as a passive isolation system, but not vice versa. For example it will become clear in the next section that a simple active controller can substitute the isolation systems of References 8, 9 and 11, 12 respectively. But no passive isolation system composed of springs, masses, and dampers, however complex and nonlinear, has all the capabilities of the active vibration control system proposed later in this paper. The principal advantages of active isolation systems are derived at least from three basic features (References 12, 13).

(1) Active systems can supply or absorb power in an arbitrary manner, while passive systems can only dissipate or temporarily store and later return energy.

(2) Active systems can produce local forces as a function of many variables some of which may be measured remotely; passive systems generate forces related to local motion variables only.

(3) Active systems can be modified as desired by servocompensators to establish certain performance specifications, passive systems do not have this possibility at all.

As pointed out in References 12 and 13, the principal disadvantages of active isolation systems compared with passive systems are derived from their need for an external power source, their possibly increased complexity and cost, and decreased reliability. But as experience with active systems grows and possibly modern microprocessor technology is maybe established for signal processing, the time will surely come when a computer controlled electrohydraulic rotor isolation system may even be superior to a passive system on a price, weight, and reliability basis. This will be, because passive rotor isolation systems need to be overdesigned as stiff, heavy structure while light, flexible, efficient structures with active control would be superior (see Reference 12 for further comments on other advantages of active isolation).

The purpose of this paper is to discuss the facilities offered by active nodal rotor isolation in comparison with existing passive systems. The paper doesn't deal with the whole MBB research program (see Reference 14) to develop an active multi-axis, multi-frequency nodal isolation system, designated as ASIS (Aktives Schwingungs-Isolations-System), but is concentrated on some essential results of the theoretical investigations for an active isolation system, which is now being developed for testing as a functional model.

2. Helicopter Vibration Control by Rotor Isolation

2.1 Rotor Isolation System - A Review

Different approaches featuring rotor isolation have been considered in the past. Conventional isolation using low natural frequency transmission suspension is applicable only with active trim devices for limiting the relative deflections of the gearbox due to large steady rotor loads. The vibration spikes in Figure 1 show that broad band isolation capability is not needed in helicopter vibration control. The task of rotor isolation is to reject the most siginificant N/rev and 2N/rev frequency disturbances which are usually responsible for component fatigue and passengers discomfort. Fuselage 1/rev vibrations due to residual unbalance and insufficient blade track are to be reduced preferably by flight balancing and tracking.

Several passive antiresonant systems have been tested, which were qualified to reduce at least the first blade passing frequency (N/rev). The focusing of the rotor/gearbox mounting (Reference 4, 5), and the nodal beam suspension of the rotor/gearbox/engine unit (Reference 6, 7) belong to a class of systems which use "natural" antiresonances for isolation purpose. These systems are difficult to tune, sensitive to parameter variations (for instance gross weight changes) and limited in application. Advanced rotors such as hingeless or bearingless rotors demand for multi-axis rotor isolation. This can be achieved by appropriate force isolators placed between the rotor/transmission unit and the fuselage. These isolators are easy to tune and produce "artificial" antiresonances for isolation purpose. Passive antiresonant force isolators have received considerable attention from the industry; notable are Kaman's DAVI (References 8, 9) and Boeing-Vertol's IRIS (References 10, 11) for single- and multi-frequent isolation respectively.

A first concept of fully active rotor nodal isolation system was developed by the Barry Wright Corporation in the late 1960's (Reference 17). The feasibility of active narrow-band isolation systems had been demonstrated in laboratory and ground tests for single-axis two-frequent isolation systems (References 18, 19 and 20). However, further studies and testing are recommended in the cited references as a means to arrive at a better understanding of multi-axis active isolation techniques in the presence of structural response of the isolated fuselage. It was claimed that active isolator performance and stability can be seriously degraded by isolated structure flexibility. Besides this pioneering work very little attention has been given to active rotor isolation devices. Therefore only Reference 2 can yet be quoted, which reports of flight tests with an active lift link in open loop control.

Quite recently modern control theory for multivariable feedback design with disturbance rejection has been developed and will prove to be a powerful tool for designing and developing active rotor isolation systems (Section 3). As an aid to understand active rotor isolation a simple mathematical helicopter model is presented in the following sections.

2.2 Rotor Nodal Isolation by Force Isolators

It has been pointed out that multi-axis, multi-frequency rotor nodal isolation systems - passive or active - are practically realized best by interposing special isolators between the transmission unit and the isolated fuselage. For simplicity a single-axis vertical rotor isolation system is selected in Figure 2 (left) with two rigid masses, one for the rotor/transmission unit and the other for the fuselage. The fixed system vertical hub forces excite the upper rotor/transmission mass. The two masses are connected by an isolator device (black box). If the isolator does not transmit any oscillatory forces to the fuselage, perfect rotor nodal isolation is achieved. That's why the black box isolator is designated as force isolator. In the case of ideal rotor isolation discrete frequency excitation forces are fully compensated chiefly by inertia forces of the oscillating rotor/transmission mass and the corresponding residual isolator output forces (rotor side, see Figure 2 right). The force isolator blocks locally the load path to the fuselage for rotor disturbances that are composed of harmonics whose frequencies are known. In practice only the isolation of the first two blade passage frequencies is necessary. The discussion of Figure 2 has made clear that rotor nodal isolation is a disturbance rejection problem.

2.3 Antiresonance Isolators and Disturbance Rejection Controllers

The crucial element in every rotor nodal isolation system is the force isolator. Due to the model of Figure 3 common unidirectional force isolators consist of the following three components:

(1) force generator

(2) spring

(3) damper .

The realization of the force generator depends on the special system, see Figure 3 (right). The well-known DAVI system uses a simple mechanical pendulum, which acts as a passive force "generator" where output are inertia forces. This concept uses a combination of opposing spring and inertia forces to create a node at the fuselage attachment point in case of antiresonance (see Reference 10). It should be noted that passive antiresonant isolators do not have the capability of opposing damping forces; that's why the parallel damper of the isolator must be kept as low as possible.

The situation is quite different for an isolator with a hydraulic servoactuator as active force generator. This element can oppose spring and damping forces at will. Therefore the active force isolator of Figure 3 can be used in principle like the DAVI element. If appropriate feedback control is used, the actuator forces oppose the equivalent spring forces, and residual damping forces guarantee system stability. Of course this controller concept is by no means adequate for active rotor isolation. Actuator non-linearities would make this "antiresonant" controller quite difficult to implement, and stability problems can yet be predicted. But there are other more effective controller concepts, which are very well suited for high performance active rotor disturbance rejection. The underlying principle of these systems with disturbance rejection feedback controllers are explained best by Figure 4. It is well-known by classical control theory that feedback systems with infinite loop gain would ideally be able to reject all disturbances from the interested output variable. Of course ideal disturbance rejection is not feasible in practice. Infinite loop gain can be achieved only for a certain class of disturbances by appropriate servo compensators. An active rotor isolation system using the concept of nodalization has to perform the following two tasks:

(1) Airframe Vibration Control by rejection of rotor induced blade passage harmonics in the operating range of rotorspeed.

(2) Transmission Deflection Control by automatic trim for limiting the steady and quasi-steady relative deflections of the rotor/transmission unit in level and maneuver flight.

Due to Figure 4 the rotor disturbance rejection problem demands for

(1) notch filter feedback of the vibration output (transmitted isolator force or acceleration at the airframe attachment point)

(2) integral feedback of the trim output (isolator deflection).

In the next section more details will be given about the underlying theory and its application to multi-axis, multi-frequency active rotor isolation system.

Typical results of a single axis (vertical axis) passive and active nodal isolation system for the helicopter BO 105 are presented in Figure 5. Comparing the amplitude response of the relative transmission deflection $|\Delta z(i\omega)|$ and force transmissibility of the isolation system $TR = |F_I(i\omega)/F_R(i\omega)|$ the characteristics of both systems are easily revealed. The passive antiresonant system (DAVI) shows its typical frequency-response with resonance peak at 24 Hz, and an antiresonance in the transmissibility plot at 28 Hz (first blade passage harmonic).

If the spring and damper data of Reference 10 are accepted, the passive system achieves the following isolation effectiveness and steady transmission deflection:

$$1 - TR = 95\% \quad \text{at } \omega = 28 \text{ Hz}$$

$$\Delta z = 1.1 \text{ mm/g at } \omega = 0$$

The two-frequency active nodal isolation system with automatic trim is designed to accomplish (theoretically) the three specifications

$$1 - TR = 100\% \quad \text{at } \omega_1 = 28 \text{ Hz}$$

$$1 - TR = 100\% \quad \text{at } \omega_2 = 56 \text{ Hz}$$

and

$$\Delta z = 0 \quad \text{at } \omega = 0 .$$

This system is free from resonance peaks, the integral controller leads to the zero at the origin of the frequency response plot (Figure 5 left) and the notch filter feedback to the two zeros in the transmissibility plot (Figure 5 right). The fuselage seems rigidly connected to the transmission with "notches" at 4/rev and 8/rev. More details about this actively controlled isolation system will be given later in the next section.

3. Active Rotor Isolation System Analysis and Design

3.1 Multivariable Feedback Theory for Disturbance Rejection

The subject of disturbance rejection by feedback controller for linear time-invariant multi-variable systems was considered recently by several authors, see References 21 through 25. An introduction to the problem of disturbance rejection and a comprehensive set of related reports are given in Reference 26. The disturbance rejection controller concept developed by Davison (References 22, 23, 24) has found to be fundamental for the analysis and design of an active rotor nodal isolation system with automatic trim. The block diagram of Figure 6 shows the basic control configuration obtained for a multi-axis two-frequency rotor isolation system with two servocompensators:

- Isolation Compensator: 4Ω - and 8Ω - notch feedback of the isolator output $\underline{y}_I$, so that asymptotically $\underline{y}_I(t) \rightarrow \underline{0}$ as $t \rightarrow \infty$. (The notches should be able to adapt rotor speed variations, i.e., automatically change their nominal centre frequency).

- Trim Compensator: Integral (0Ω-notch) feedback of the trim output $\underline{y}_T$, so that asymptotically $\underline{y}_T(t) \rightarrow \underline{\delta}_{ref}$ as $t \rightarrow \infty$.

This control concept may be interpreted as being a generalization of the single-input single-output disturbance rejection solution (Figure 4) to multivariable systems.

To recapitulate the fundamental properties of the control system of Figure 6 are the following:

1. The controller is of feedback type.

2. The feedback loop incorporates a model of the dynamic system which generates the external disturbances to be rejected.

It has been shown that these are necessary features of any controller which has to be "robust" (Reference 22) or "structurally stable" (Reference 27).

The existance of a solution for the stated twofold rotor disturbance rejection problem can be established by necessary and sufficient conditions given in Reference 22, too.

In practice the complete state of the isolation system is generally not available by measurement, and the control concept of Figure 6 must be augmented by a stabilizing compensator as indicated in the block diagram of Figure 7. The sole purpose of the stabilizing compensator is to stabilize the augmented system obtained by applying the servocompensator to the plant (see References 23 and 24). (It must be noted that due to Davison the integrator and notch outputs may be added to the input of the stabilizing compensator from Figure 7 also). The practical feasibility of the modified control configuration (Figure 7) with output feedback depends upon the complexity this stabilizing compensator is needed for. The possibility of simple output feedback without an additional compensator for stabilizing will be discussed later.

3.2 State Equations of a Single-Axis Active Rotor Isolation System

For better understanding of the theory discussed before the plant equations for the simple single-axis vertical rotor isolation system with rigid masses will be given. The linearized equations for an electrohydraulic force isolator are presented in Table 1. By proper selection of the hydraulic components (Reference 28)

- servoactuator with high hydraulic stiffness
- servovalve with high natural frequency
- bypass for lowering the actuator pressure gain

it is possible to reduce the actuator equations to that of an "ideal" force generator with an equivalent linear (hydraulic) damper in parallel (Table 1 bottom). This reduction can be established mathematically by the so-called singular perturbation method, see Reference 29. This method actually leads to a complete separation of slow and fast system modes. It can be used very effectively for control system design.

Table 2 contains the dimensionless state equations of the single-axis helicopter isolation system. The "design model" is based on the reduced force isolator equations and is suited for the control system synthesis, whereas the "simulation model" uses the complete isolator equations. With the reference quantities

$$\delta_o = 0.0025\ \text{m}, \quad \Delta p_{max} = 2.06 \cdot 10^7\ \text{N/m}^2,$$

$$i_{max} = 10\ \text{mA, and} \quad \Omega = 44.4\ \text{rad/s} \mathrel{\hat{=}} 7\ \text{Hz}$$

the following nondimensional values for Table 2 are obtained:

$\bar{\omega}_\Delta = 125.70$, $\zeta_\Delta = 0.005$, $\bar{\omega}_{SV} = 1257.0$, $\zeta_{SV} = 0.5$,
$\bar{\omega}_A = 2288.49$, $\bar{\tau}_A = 6.97 \cdot 10^{-4}$, $\bar{k}_\Delta = 0.61185$, $\bar{d}_\Delta = 0.00216$,
$M = 0.1519$, $\gamma = 34.832$, $\delta = 1.9898$, $\bar{A} = 2.659$,
$\bar{K}_\varepsilon = 0.6644$, $\bar{K}_i = 6.413 \cdot 10^{-5}$

3.3 Control System Design by Linear Optimal Control Theory

For active vibration isolation the Optimal Control Method is especially suitable because of the possibilities offered by weighting factors for state and control variables (see Reference 12). One can easily find stable control systems with the desired performance without excessive values of auxiliary variables.

For a linear control system with the state $\underline{x}$ and the control input $\underline{u}$ the quadratic performance criterion

$$J = \int_0^\infty (\underline{x}^T \underline{Q} \underline{x} + \underline{u}^T \underline{H} \underline{u}) dt$$

has to be minimized. The solution of the corresponding Riccati equation leads to a constant linear feedback controller. Thus, one can obtain a fast response with large control forces or a slower response with lower control forces (see Reference 30).

The actual control system is illustrated in Figure 8. As shown in the previous section the complete mathematical (simulation) model can be reduced to a simpler system (design model) by neglecting the actuator dynamics, so that only the isolator deflection Δz, its derivative $\Delta\dot{z}$, the integrator variable n_0, and the notch variables n_1, $\dot{n}_1$, n_2, and $\dot{n}_2$ have to be controlled.

The problem was now to find appropriate weighting factors for the diverse variables. As a first attempt all variables were weighted equally with the factor 1 with the exception of $\Delta\dot{z}$, which got the weighting factor 0.001 because of its lower importance. With the special MBB computer program REGEL ("computer aided design") the controller coefficients have been found. The excellent time behaviour of this "first attempt controller" can be seen on the Figures 9 and 10. Figure 9 shows that at a harmonic disturbance the isolator deflection Δz reaches a stable oscillation after 3 cycles; the isolator force F_I vanishes after ca. 4 cycles i.e. 1 rotor revolution or 1/7 sec. The similarily fast response of the notch variables n_1 and n_2 is shown on Figure 9 right. A test maneuver ramp load of 1.5 g in 0.5 sec yields the response of Δz and F_I given in Figure 10 left. The trim integrator limits the isolator deflection to less than 6% of the maximal actuator stroke (= ±2.5 mm). The isolator force reaches the value of 1.5 g times $m_F/(m_F + m_R)$. A unit step deflection (Figure 10 right) shows the good tracking behaviour of this Optimal Controller.

The frequency response of Δz and F_I has been presented already in Figure 5 in comparison with the DAVI results. The vibration isolation can directly be seen from the solid line in the force transmissibility plot ($TR = |F_I/F_R|$). Oscillations with the frequency of 4Ω and 8Ω are completely canceled, but the bandwidth of the isolation is not very large (as reference value TR = 0.1 or 90% isolation is taken). So the main criterion of this controller design is not the time behaviour but the frequency response. For spreading the isolation band-width the notch variables were weighted with higher factors. Figure 11 (right) shows for example that with a weighting of 1000 a very broad vibration isolation can be obtained. The limit of these possibilities is reached, when this controller is connected to the complete simulation model, because stability problems arise with such a high gain controller. A compromise between stability of the simulation model and band-width of the isolation can be found by weighting the control input appropriately. Figure 11 (left) shows the transmissibility for the weighting values $\underline{Q}$ = diag (1, 0.001, 1, 1000, 1000, 1000, 1000) and H = 100.

The use of Optimal Control Theory for active nodal isolation of flexible structures calls for a special stability compensator (see Figure 7) known as state observer, possibly with disturbance estimation. This problem had been investigated in References 31 and 32.

3.4 The Energy Controller - A Liapunov Concept for Active Rotor Isolation

In order to overcome the difficulties of active rotor nodal isolation in presence of structure flexibility Laier has proposed (Reference 33) a control concept based on the Second Method of Liapunov (see References 34 and 35). The corresponding block diagram is shown in Figure 12 for a multi-axis two-frequency active nodal isolation system completed by an integral trim feedback. For the analysis of this concept the knowledge of an appropriate Liapunov function is necessary. In Table 3 a Liapunov function is generated by using the Hamiltonian function of the whole system. The derived "Energy Controller" stabilizes the resulting system by the following three feedback loops:

$\underline{y}_L$ - position feedback,

$\dot{\underline{y}}_L$ - velocity feedback,

and eventually $\ddot{\underline{y}}_L$ - acceleration feedback,

where $\underline{y}_L = \underline{\delta} - \sum_{\nu} \underline{\alpha}_{\nu} \, \underline{n}_{\nu} \qquad (\nu = 1,2)$

is the difference of the isolator deflection $\underline{\delta}$ and a weighted sum of the notch variables $\underline{n}_1$ and $\underline{n}_2$. The new vector $\underline{y}_L$, designated as Liapunov output signal, and its two derivatives must be available by measurement etc. The input to the plant (helicopter) and notches (undamped oscillators) are the signals $\underline{F}_I$ of the transmitted isolator forces and are not the accelerations $\underline{a}_I$ at the corresponding airframe attachment points. For an ideal rigid fuselage both feedback signals are clearly proportional (see Table 2), but this is no longer the case for real flexible helicopter airframe structures, see Reference 18.

If the second order matrix differential equations are transformed into first order state equations, the Liapunov control concept of Figure 12 accepts in principle the form of Davison's control configuration (Figure 7) with

- simple output feedback control (No stabilizing compensator necessary!)
- "feedforward control" in case of acceleration feedback (No measurement of rotor disturbances necessary!)

In summary the "Energy Controller" is a new concept in active rotor nodal isolation. Taking advantage of the special structure of the plant equations, this concept can tolerate structure flexibility and does not need any stabilizing compensator. The implementing of trim loop may result in some stability problems. This possible difficulty can be overcome by using a parallel spring to the isolator with sufficient stiffness.

3.5 Control System Design by the Second Method of Liapunov

It has just become practical to synthesize an active rotor nodal isolation system in the time domain due to the Liapunov concept of Table 3 by computer aided design. Therefore, first results for a single-axis helicopter model with

(1) rigid fuselage mass,

and (2) flexible fuselage structure modelled by four symmetric modes with natural frequencies at 7, 27, 75, and 163 Hz

can be presented now. All the controllers were computed with a modified version of the program REGEL mentioned in an earlier section. The actual control system is illustrated in Figure 13. For reason of simplicity the acceleration loop has been omitted. During the design process

three controller coefficients K_{L_0}, K_{L1} and $K_{0\Omega}$ (all positive),

and two notch-weights α_1, α_2 (both positive)

had to be adjusted appropriately. To assess the effect of flexibility of the isolated fuselage mass, Figure 14 compares related time histories of the transmitted isolator force $F_I/(m_{tot} \cdot g)$ and the corresponding isolator attachment acceleration $\ddot{z}_F/g$ due to a cosine rotor disturbance. The 4Ω- and 8Ω-rotor forces start at time t = 0. From Figure 14 (left) one can easily find that in case of a rigid airframe the computed force and acceleration are proportional, as expected, and are quickly rejected by the controller. More interesting are the plots for the model with airframe flexibility, see Figure 14 (right). Using the same "Energy Controller", the transmitted isolator force is rejected as before, whereas the airframe acceleration is not. This result impressingly demonstrates, what active rotor nodal isolation by the Liapunov concept really means:

Active rejection of rotor disturbances, but not active control of the airframe vibration modes.

That's why the airframe vibrations are suppressed mainly by structural damping. Figure 15 continues the comparison of the system with and without airframe flexibility in the frequency domain. As expected, the force transmissibility of both systems is nearly equal except for the disturbing effect of the first mode (natural frequency in the vicinity of 1/rev). Further investigations will probably confirm the applicability of the Liapunov Controller for active rotor nodal isolation in case of real flexible airframe structures.

4. Multi-Axis Rotor Isolation Concept

Reference 14 gives an active rotor nodal isolation concept for the helicopter BO 105 with application of multivariable feedback rejection controllers (Figure 6). By use of the rigid-body model of Figure 16 the performance of a three-channel isolation system has been investigated. Figure 17 shows for example the force transmissibility "matrix" for nodal isolation of 4Ω-disturbances in the horizontal, vertical, and pitch axis. The controller was designed by Optimal Control Theory; better results could be achieved simply by changing the weighting factors. It should be noted that, in principle, multi-axis system synthesis presents no special difficulty for modern state-variable technique.

For the purpose of research and development the following isolation system has been defined for the helicopter BO 105 (see Figure 18):

- isolation axis	:	5 (yaw axis unisolated)
- nodal frequencies	:	4/rev, 8/rev
- servoactuators (balanced)	:	3 vertical, 2 horizontal
- servovalves	:	electrohydraulic
- hydraulic supply	:	high-pressure power package (3000 psi)
- notch filters	:	adaptive for rotor speed variation
- transmission trim	:	automatic
- controller	:	DDC (microprocessor)
- sensors (for each isolator)	:	relative displacement, differential pressure, and acceleration (if needed)
- fail-safe precautions	:	shutoff device, spring support

A summary of estimated power, weight, and cost for this system is included in the tables of Figure 18.

5. Laboratory Research Model

The Laboratory Research Model (Figure 19) was defined for investigations of one vertical channel of an active isolation system, in particular of the electrohydraulic actuator in connection with different control concepts.

Scaling

Since three equal actuators are provided for the helicopter vertical axis, the size of the model may be reduced using only one actuator and scaling the mass values (1 : 3). This results in

Fuselage + Actuator	:	670 kg
Rotor	:	120 kg
Σ	:	790 kg $= \frac{1}{3}\, m_{tot}$.

Description

- The helicopter is simulated by two symmetric bodies, of which the middle one simulates the fuselage and the outer one the transmission and rotor system. The latter was designed as a framework in order to ensure suspension as well as excitation with available implements. While the rotor/transmission mass of the model is a rigid body, the fuselage mass is designed both as rigid and as flexible body.
- The two bodies are connected by the actuator and two parallel support springs.
- Rotor-disturbances are simulated by an electrodynamic shaker.
- In order to ensure only small deviations from the free-free flight vibration state, the rotor/transmission system is suspended on a very soft spring (air spring).
- For preventing displacements in the horizontal axis the two bodies are lead by auxiliary springs with low system frequencies in the vertical and high frequencies in the horizontal axis.

Actuator, Servovalve

In order to realize the nodal isolation concept, all system components - actuator, servovalve, and sensors - have to satisfy special requirements. Surely the critical component is the servoactuator, which should have dry break-out friction less than 200 N (equiv. 1% max. load).

Actuator (fabricated by HAENCHEN, Stuttgart):

stroke	:	± 0.25 cm
piston-area (balanced)	:	10.0 cm^2
max. flow	:	150 cm^3/s ≙ 9 cis

supply pressure	:	206 bar ≙ 3000 psi
dry break-out friction	:	< 200 N

Servovalve, flow controlled (MOOG, Type 30, Standard Series 31):

max. pressure	:	206 bar ≙ 3000 psi
max. flow	:	≃ 430 cm^3/s ≙ 26 cis
linearity	:	< ± 7%
hysteresis	:	< 3%
threshold	:	< 0.5%

Sensors

The principal sensors are:

- relative displacement transducer
- accelerometer and load cell respectively (in series with actuator).

Because of some difficulties, using a load cell for measuring the transmitted isolator force, a differential pressure transducer is provided for "computing" the F_I-signal.

Data:

Differential Pressure Transducer (Standard Controls Inc., 210-60-090)

nonlinearity/hysteresis	:	0.25%
repeatability	:	0.1%
pressure range	:	± 3000 psi

Relative Displacement Transducer (TWK, IW10)

linearity	:	0.5%

Accelerometer (Sundstrand Data Control Inc., QA 1000)

linearity	:	0.03%
hysteresis	:	0.001%
repeatability	:	0.003%

The laboratory tests will show, whether rotor disturbance compensation by inertia forces for both blade passage harmonics can be realized. The following data gives an impression of the practical problems (see Figure 5):

transmission displacement at 4Ω = 28 Hz	:	2.0 mm/g
transmission displacement at 8Ω = 56 Hz	:	0.5 mm/g

Typical vertical loads for maneuver:

4Ω : $\bar{F}_R = \pm 0.13\ g \rightarrow \Delta z = \pm 0.26$ mm

8Ω : $\bar{F}_R = \pm 0.052\ g \rightarrow \Delta z = \pm 0.03$ mm

Advanced hydraulic technology will probably be able to handle actuator oscillations of such small values.

6. Conclusions

The following conclusions can be drawn from the results of the ASIS research program:

- Modern state-variable technique for disturbance rejection controllers is a powerful tool for analysis and design of multi-axis, multi-frequency active rotor nodal isolation systems.
- Structural flexibility can be tolerated by the so-called "Energy Controller". This control concept, based on the Second Method of Liapunov, takes advantage of the special structure of the plant equations, and does not demand for stabilizing compensators in case of output feedback.
- The worked-out concept will now be tested in a laboratory research model, and subsequent flight tests have to be made.
- The performance of active rotor isolation is superior to any existing passive device.
- The principal disadvantages of active rotor isolation systems compared with passive ones are their complexity and cost.
- However, actively controlled hydraulic servoelements - probably in connection with advanced microprocessor technology - will surely be the solution of the helicopter vibration problem.

7. References

1. D.E. Brandt, Vibration control in rotary-winged aircraft, AGARD Meeting on Helicopter Developments, Jan. 1966

2. D.L. Kidd, R.W. Balke, W.F. Wilson and R.K. Wernicke, Recent advances in helicopter vibration control, 26th Annual National Forum of the American Helicopter Society, Paper No 415, June 1970

3. D.E.H. Balmford, The control of vibration in helicopters, The Aeronautical Journal of the Royal Aeronautical Society, Feb. 1977

4. F.L. Legrand, Structural solutions investigated in connection with the vibration problems in the SA 330, 24th Annual National Forum of the American Helicopter Society, Paper No 224, May 1968

5. C.W. Hughes and R.K. Wernicke, Flight test of a hingeless flexbeam rotor system, USAAMRDL-TR-74-38, June 1974

6. D.P. Shipman, J.A. White and J.D. Cronkhite, Fuselage nodalization, 28th Annual National Forum of the American Helicopter Society, Paper No 611, May 1972

7. D.P. Shipman, Nodalization applied to helicopters, National Aerospace Engineering and Manufacturing Meeting, Paper No 730893, Oct. 1973

8. R. Jones, A full-scale experimental study of helicopter rotor isolation, USAAVLABS-TR-71-17

9. A.D. Rita, J.H. McGarvey and R. Jones, Helicopter rotor isolation evaluation utilizing the dynamic antiresonant vibration isolator, 32nd Annual National V/STOL Forum of the American Helicopter Society, Paper No 1030, May 1976

10. R.A. Desjardins and W.E. Hooper, Rotor isolation of the hingeless rotor BO 105 and YUH-61 helicopters, 2nd European Rotorcraft and Powered Lift Aircraft Forum, Paper No 13, Sept. 1976

11. W.E. Hooper and R.A. Desjardins, Anti-resonant isolation for hingeless rotor helicopters, Aerospace Engineering and Manufacturing Meeting, Paper No 760893, Dec. 1976

12. D.C. Karnopp, Active and passive isolation of random vibration, ASME Design Engineering Technical Conference, Sept. 73

13. J.K. Hedrick and D.N. Wormley, Active suspensions for ground transport vehicles - a state of the art review, The Winter Annual Meeting of the American Society of Mechanical Engineers, Nov. 1975

14. H. Strehlow, H. Habsch, W. Hagemann and G. Seitz, Aktives Schwingungsisolationssystem ASIS - Konzeptuntersuchungen und Systemdefinition, Messerschmitt-Bölkow-Blohm GmbH Bericht UD-188-76

15. P.W. von Hardenberg and P.B. Saltanis, Preliminary development of an active transmission isolation system, 27th Annual National V/STOL Forum of the American Helicopter Society, Paper No 514, May 1971

16. P.W. von Hardenberg and P.B. Saltanis, Ground test evaluation of the Sikorsky active transmission isolation system, AD 736347, Sept. 1971

17. P.C. Calcaterra and D.W. Schubert, Isolation of helicopter rotor-induced vibrations using active elements, AD 859806, June 1969

18. J.E. Ruzicka and D.W. Schubert, Recent advances in electrohydraulic vibration isolation, The Shock and Vibration Bulletin 39, Part 4, April 1969

19. R.E. Allen and P.C. Calcaterra, Design, fabrication and testing of two electrohydraulic vibration systems for helicopter environments, NASA CR-112052

20. B.R. Hanks and W.J. Snyder, Ground tests of an active vibration isolation system for a full-scale helicopter, The Shock and Vibration Bulletin 43, Part 4, June 1973

21. C.D. Johnson, Accommodation of external disturbances in linear regulator and servomechanism problems, IEEE Transactions on Automatic Control, Vol. AC-16, No 6, Dec. 1971

22. E.J. Davison, The output control of linear time-invariant multivariable systems with unmeasurable arbitrary disturbances, IEEE Transactions on Automatic Control, Vol. AC-17, No 5, Oct. 1972

23. E.J. Davison and A. Goldenberg, Robust control of a general servomechanism problem: The servo compensator, 6th IFAC Congress, August 1975

24. E.J. Davison, The robust decentralized control of a general servomechanism problem, IEEE Transactions on Automatic Control, Vol. AC-21, No 1, Feb. 1976

25. P.C. Müller and J. Lückel, Optimal multivariable feedback system design with disturbance rejection, Automatica 12, 76

26. G. Weihrich, Mehrgrößenzustandsregelung unter Einwirkung von Stör- und Führungssignalen: Einführung und Überblick, VDI/VDE-Aussprachetag "Regelungssynthese im Zustandsraum", Feb. 1977

27. W.M. Wonham, Linear multivariable control, Springer-Verlag, Berlin 1974

28. E. Göllner, Lineare regelungstechnische Analyse elektrohydraulischer Kraftregelungen, Ölhydraulik und Pneumatik 19, No 12, 1975

29. J.H. Chow and P.V. Kokotović, A decomposition of near-optimum regulators for systems with slow and fast modes, IEEE Transactions on Automatic Control, Oct. 1976

30. H. Kwakernaak and R. Sivan, Linear optimal control systems, Wiley - Interscience New York, 1972

31. G. Schulz, Konzepte zur Auslegung eines voll-aktiven Hubschrauber-Schwingungsisolationssystems mittels Ausgangsvektorrückführung, DFVLR Oberpfaffenhofen, Sept. 1976

32. G. Schulz and G. Kreißelmeier, Aktive Schwingungsisolation bei einem Hubschrauber, VDI/VDE-Aussprachetag "Regelungssynthese im Zustandsraum", Feb. 1977

33. W. Laier, Der Energieregler und seine numerische Anwendung auf die vollaktive Hubschrauberschwingungsisolation - ein Liapunov-Regelkonzept, Messerschmitt-Bölkow-Blohm GmbH, Technische Niederschrift TN GDT1-1/77

34. R.E. Kalman and J.E. Bertram, Control system analysis and design via the "Second Method" of Liapunov, ASME-AIEE-IRE-ISA National Automatic Control Conference, Paper No 59-NAC-2, Nov. 1959

35. A.M. Letov, Stability theory, In: System Theory ed. by L.A. Zadeh / E. Polak, McGraw-Hill, 1969

	LINEAR MODEL OF A HYDRAULIC FORCE ACTUATOR WITH ACTUATOR DYNAMICS
SERVOVALVE FLOW	$q = K_\varepsilon \cdot \varepsilon - K_p \cdot \Delta p$
ACTUATOR FLOW	$q = A \cdot \Delta\dot{z} + A^2/k_{oil} \cdot \Delta\dot{p} + C_L \cdot \Delta p$
SERVOVALVE SPOOL STROKE	$\ddot{\varepsilon} + 2 \cdot \zeta_{SV} \cdot \omega_{SV} \cdot \dot{\varepsilon} + \omega_{SV}^2 \cdot \varepsilon = \omega_{SV}^2 \cdot K_i \cdot i$
PISTON AREA	$A = A_R = A_F$
ISOLATOR FORCE	$F_I = k_\Delta \cdot \Delta z + d_\Delta \cdot \Delta\dot{z} - A \cdot \Delta p$
	LINEAR MODEL OF A HYDRAULIC FORCE ACTUATOR WITHOUT ACTUATOR DYNAMICS
APPROXIMATIONS	$\omega_{SV} \to \infty \;;\; k_{oil} \to \infty$
LOAD PRESSURE DIFFERENCE	$\Delta p = \frac{K_\varepsilon \cdot K_i}{K_p + C_L} \cdot i - \frac{A}{K_p + C_L} \cdot \Delta\dot{z}$
ISOLATOR FORCE	$F_I = k_\Delta \cdot \Delta z + \left(d_\Delta + \frac{A^2}{K_p + C_L} \right) \cdot \Delta\dot{z} - A \frac{K_\varepsilon \cdot K_i}{K_p + C_L} \cdot i$

NOTATIONS	
K_ε	flow gain
K_p	flow pressure coefficient
Δp	pressure difference
k_{oil}	oil compressibility
C_L	leakage flow coefficient
ζ_{SV}	damping ratio of the servovalve
ω_{SV}	natural frequency of the servovalve
K_i	electric gain
i	signal current
k_Δ	parallel spring
d_Δ	parallel damper

TABLE 1: EQUATIONS FOR AN ELECTROHYDRAULIC FORCE ISOLATOR

	PLANT WITH ACTUATOR DYNAMICS (Simulation Model)	PLANT WITHOUT ACTUATOR DYNAMICS (Design Model)
STATE	$\underline{x}_p^T = [\Delta\bar{z}, \Delta\bar{z}', \bar{\varepsilon}, \bar{\varepsilon}', \Delta\bar{p}]$	$\underline{x}_p^T = [\Delta\bar{z}, \Delta\bar{z}']$
PLANT	$\underline{A}_p = \begin{bmatrix} 0 & 1 & 0 & 0 & 0 \\ -\frac{\bar{\omega}_A^2}{1-M} & -\frac{2\zeta_A\bar{\omega}_A}{1-M} & 0 & 0 & \frac{Y}{1-M} \\ 0 & 0 & 0 & 1 & 0 \\ 0 & 0 & -\bar{\omega}_{sv}^2 & -2\zeta_{sv}\bar{\omega}_{sv} & 0 \\ 0 & -\frac{\bar{\omega}_A^2}{Y}(1-M) & \bar{K}_\varepsilon\frac{\bar{\omega}_A^2}{Y}(1-M) & 0 & -\frac{1}{\bar{\tau}_A} \end{bmatrix}$	$\underline{A}_p = \begin{bmatrix} 0 & 1 \\ 0 & 0 \end{bmatrix}$
CONTROL INPUT	$\underline{b}_p^T = [0, 0, 0, \bar{\omega}_{sv}^2 \bar{K}_I, 0]$	$\underline{b}_p^T = [0, \frac{\delta}{(1-M)M}]$
DISTURBANCE INPUT	$\underline{w}_p^T = [0, \delta/M, 0, 0, 0]$	$\underline{w}_p^T = [0, \delta/M]$
OUTPUT	$\underline{C}_p = \begin{bmatrix} 1 & 0 & 0 & 0 & 0 \\ \bar{K}_\varepsilon & \bar{d}_\varepsilon & 0 & 0 & -\bar{A} \end{bmatrix}, \underline{d}_p = \begin{bmatrix} 0 \\ 0 \end{bmatrix}$	$\underline{C}_p = \begin{bmatrix} 1 & 0 \\ 0 & 0 \end{bmatrix}, \underline{d}_p = \begin{bmatrix} 0 \\ 1 \end{bmatrix}$
TRANSFORMATION	$\underline{T}_p = \begin{bmatrix} 1 & 0 \\ 0 & \frac{\delta}{1-M} \end{bmatrix}$	$\underline{T}_p = \begin{bmatrix} 1 & 0 \\ 0 & \frac{\delta}{1-M} \end{bmatrix}$
OUTPUT / CONTROL / REFERENCE } SIGNAL	$\underline{y}_p^T = [\Delta\bar{z}, \bar{F}_I], \quad u = \bar{\varepsilon}, \quad r = \Delta\bar{z}_{ref}$	$\underline{y}_p^T = [\bar{z}, \bar{F}_I], u = \bar{F}_I, r = \Delta\bar{z}_{ref}$

TABLE 2: STATE EQUATIONS FOR A SINGLE-AXIS RIGID ROTOR ISOLATION SYSTEM

HELICOPTER (rigid body modes eliminated) ω_ν - notches (weighted notch variables)	$\underline{M}\cdot\ddot{\underline{q}} + \underline{D}\cdot\dot{\underline{q}} + \underline{K}\cdot\underline{q} = \underline{B}_q\cdot\underline{F}_I + \underline{W}_q\cdot\underline{F}_p$ $\underline{M}_\nu\cdot(\ddot{\underline{\eta}}_\nu + \omega_\nu^2\underline{\eta}_\nu) = \underline{\hat{A}}_\nu\cdot\underline{F}_I \; ; \; \underline{\eta}_\nu := \underline{M}_\nu^{-1}\cdot\underline{\xi}_\nu$
LIAPUNOV - OUTPUT (def.)	$\underline{y}_L := \underline{\delta} - \sum\underline{\Delta}_\nu\cdot\underline{\eta}_\nu \; ; \; \underline{\delta} := \underline{C}_q\cdot\underline{q} \; ; \; \underline{C}_q = -\underline{B}_q^T \; ; \; \underline{\Delta}_\nu = \underline{\hat{A}}_\nu\cdot\underline{M}_\nu^{-1}$
LIAPUNOV FUNCTION	$V = \frac{1}{2}\cdot(\dot{\underline{q}}^T\cdot\underline{M}\cdot\dot{\underline{q}} + \underline{q}^T\cdot\underline{K}\cdot\underline{q}) +$ $\frac{1}{2}\cdot\sum_\nu(\dot{\underline{\xi}}_\nu^T\cdot\underline{M}_\nu\cdot\dot{\underline{\xi}}_\nu + \omega_\nu^2\cdot\underline{\xi}_\nu^T\cdot\underline{M}_\nu\cdot\underline{\xi}_\nu) +$ $\frac{1}{2}\cdot(\dot{\underline{y}}_L^T\cdot\underline{K}_{L_2}\cdot\dot{\underline{y}}_L + \underline{y}_L^T\cdot\underline{K}_{L_0}\cdot\underline{y}_L)$ $\dot{V} = -\dot{\underline{q}}\cdot\underline{D}\cdot\dot{\underline{q}} - \dot{\underline{y}}_L^T\cdot(\underline{F}_I - \underline{K}_{L_2}\cdot\ddot{\underline{y}}_L - \underline{K}_{L_0}\cdot\underline{y}_L)$
LIAPUNOV - CONTROLLER (ENERGY - CONTROLLER)	IF $\underline{F}_I := \underline{K}_{L_0}\cdot\underline{y}_L + \underline{K}_{L_1}\cdot\dot{\underline{y}}_L + \underline{K}_{L_2}\cdot\ddot{\underline{y}}_L \; ; \; \underline{K}_{L_0}\geq 0, \; \underline{K}_{L_1} > 0, \; \underline{K}_{L_2}\geq 0$ THEN V = positive-definite AND $\dot{V}$ = negative-definite

TABLE 3: ENERGY - CONTROLLER FOR AN ACTIVE ROTOR NODAL ISOLATION SYSTEM BY LAIER

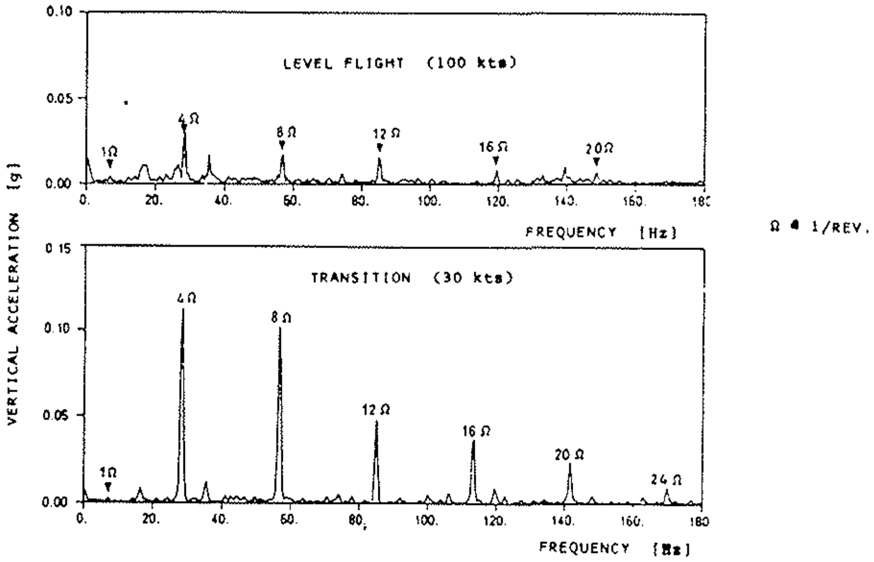

FIGURE 1: AMPLITUDE SPECTRA AT THE PILOT SEAT (BO 105)

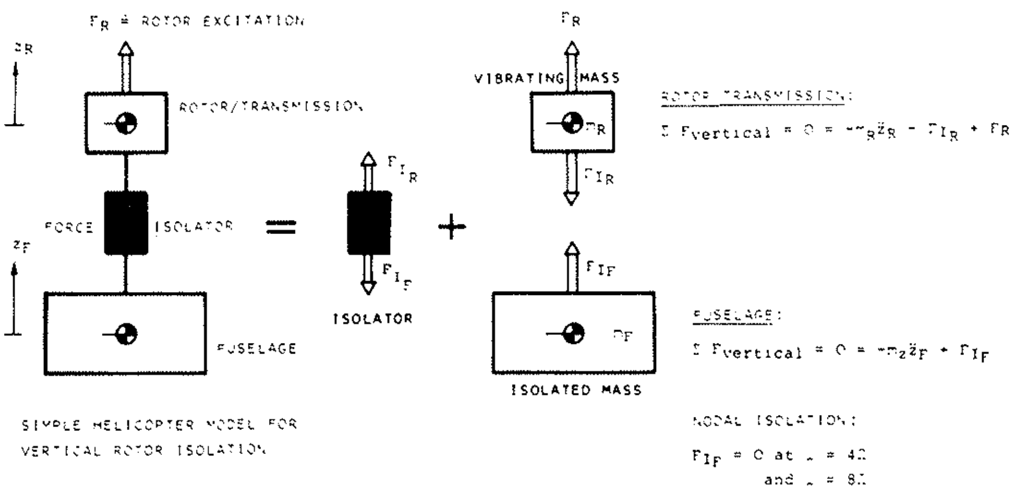

FIGURE 2: PRINCIPLE OF ROTOR NODAL ISOLATION

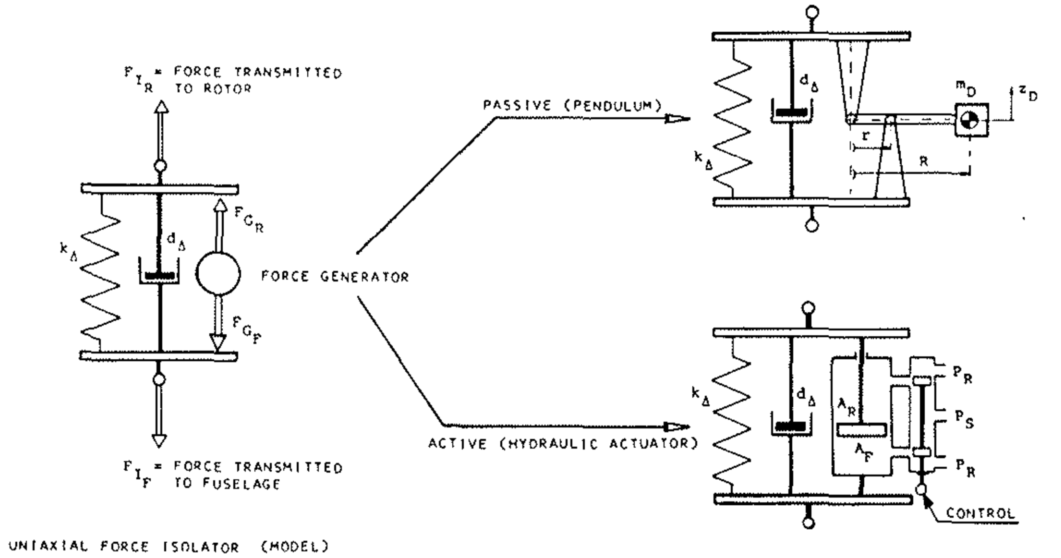

FIGURE 3: REALISATION OF PASSIVE AND ACTIVE FORCE ISOLATORS

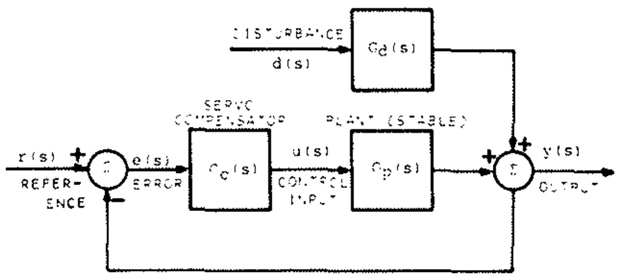

DISTURBANCE TRANSFER FUNCTION:

$$\frac{y(s)}{d(s)} = \frac{G_d(s)}{1 + G_c(s) \cdot G_p(s)}$$

	SERVO COMPENSATOR	DISTURBANCE TRANSFER FUNCTION	ASYMPTOTIC SOLUTION
IDEAL DISTURBANCE REJECTION BY INFINITE GAIN (NOT REALIZABLE)	$G_c(s) = K \to \infty$	$\frac{y(s)}{d(s)} = \frac{G_d(s)}{1 + K \cdot G_p(s)}$	for all d(s): $y \to 0$ for $K \to \infty$
REJECTION OF CONSTANT DISTURBANCES BY INTEGRATOR	$G_c(s) = \frac{1}{s}$	$\frac{y(s)}{d(s)} = \frac{s \cdot G_d(s)}{s + G_p(s)}$	for $d(s) = 1/s$: $\lim_{t \to \infty} y(t) = \lim_{s \to 0} s \cdot y(s) = 0$
REJECTION OF SINUSOIDAL DISTURBANCES BY NOTCH FILTER	$G_c(s) = \frac{1}{s^2 + \omega_v^2}$	$\frac{y(s)}{d(s)} = \frac{(s^2 + \omega_v^2) \cdot G_d(s)}{s^2 + \omega_v^2 + G_p(s)}$	for $d(s) = \omega_v/(s^2 + \omega_v^2)$: $\lim_{t \to \infty} y(t) = \lim_{s \to 0} s \cdot y(s) = 0$

FIGURE 4: DISTURBANCE REJECTION BY FEEDBACK CONTROLLERS (PRINCIPLE)

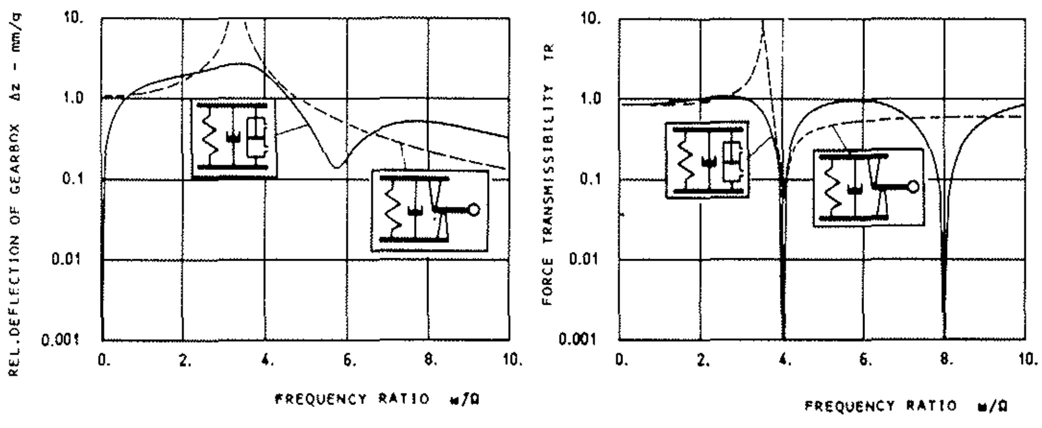

FIGURE 5: TYPICAL FREQUENCY RESPONSE OF ACTIVE AND PASSIVE ROTOR NODAL ISOLATION (VERTICAL AXIS, BO 105)

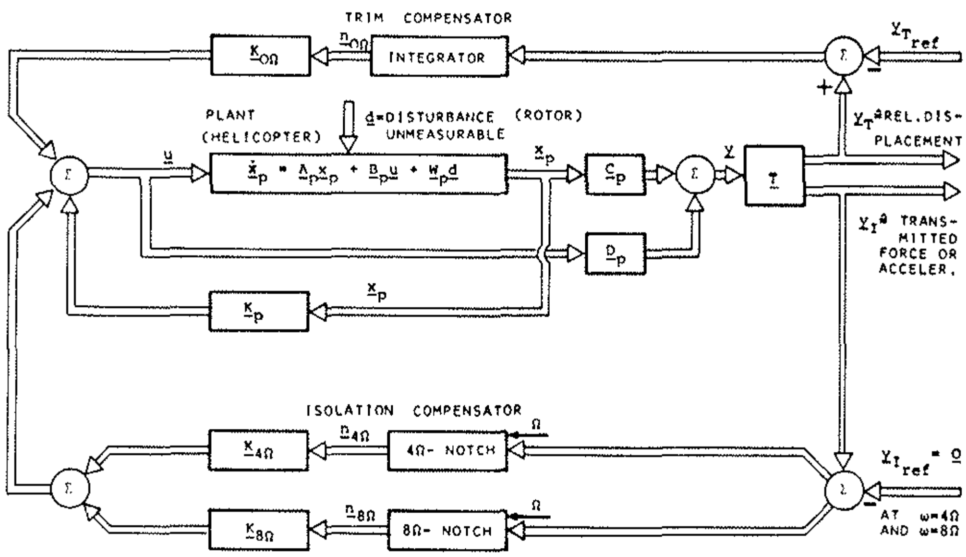

FIGURE 6: CONTROL CONFIGURATION FOR AN ACTIVE HELICOPTER ISOLATION SYSTEM IF THE COMPLETE STATE IS AVAILABLE (DAVISON)

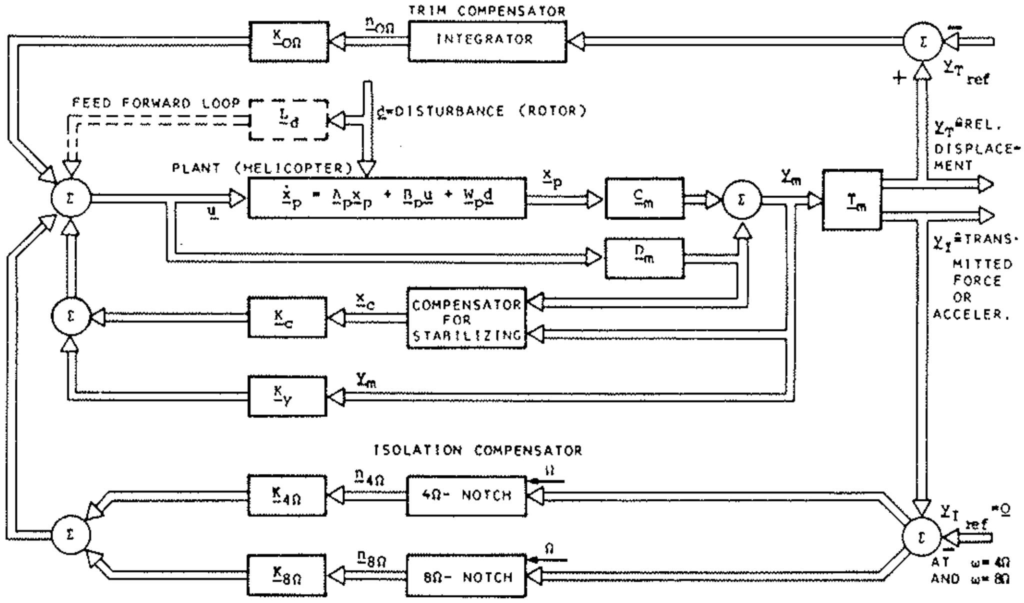

FIGURE 7: CONTROL CONFIGURATION FOR AN ACTIVE HELICOPTER ISOLATION SYSTEM IF THE STATE IS PARTIALLY MEASURABLE (DAVISON)

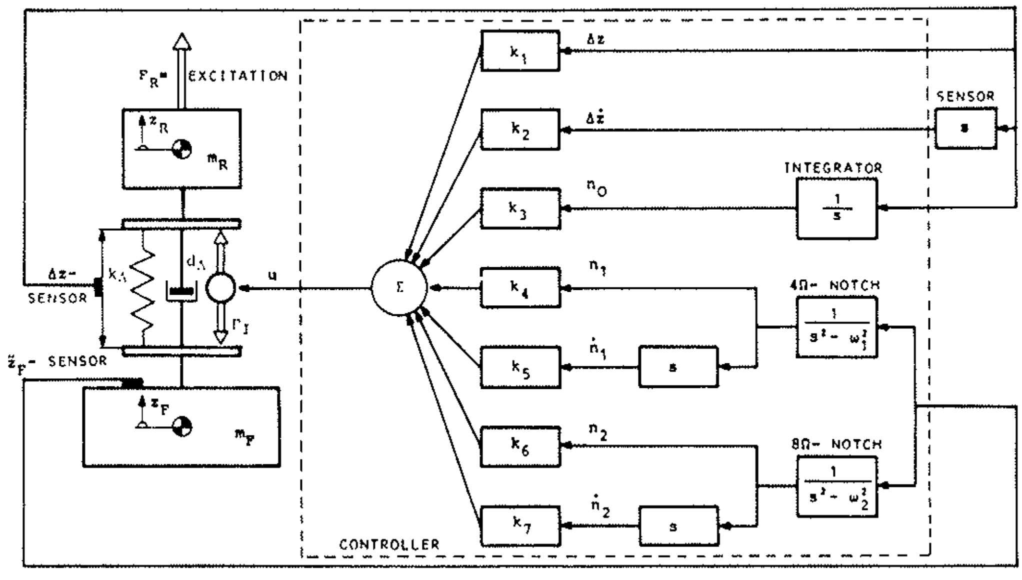

FIGURE 8: ACTIVE ISOLATION SYSTEM FOR THE VERTICAL AXIS WITH STATE VARIABLE FEEDBACK

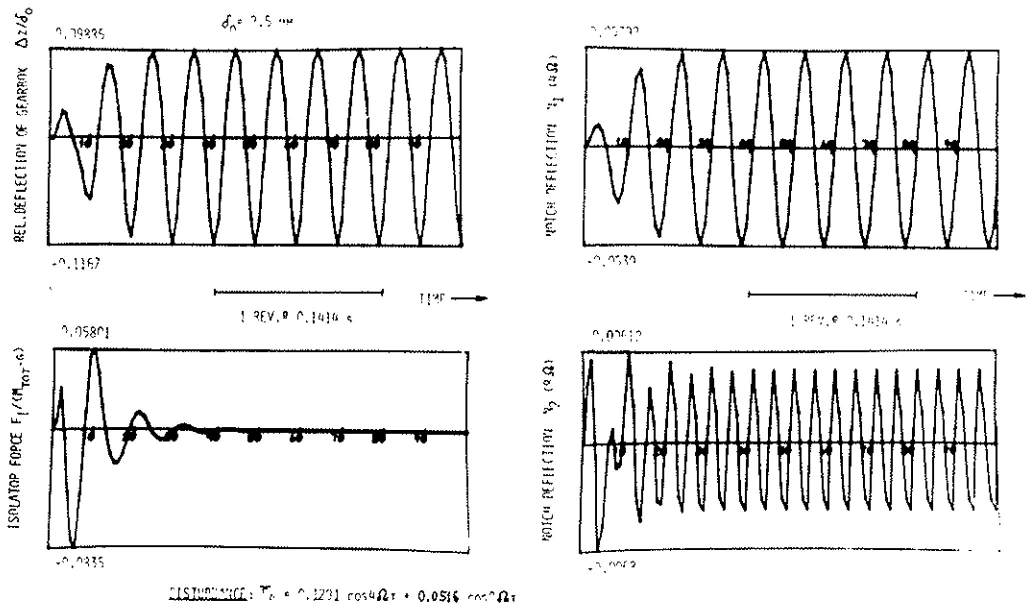

FIGURE 9: OPTIMAL CONTROLLER RESPONSE ON HARMONIC ROTOR DISTURBANCE (VERTICAL AXIS, BO 105)

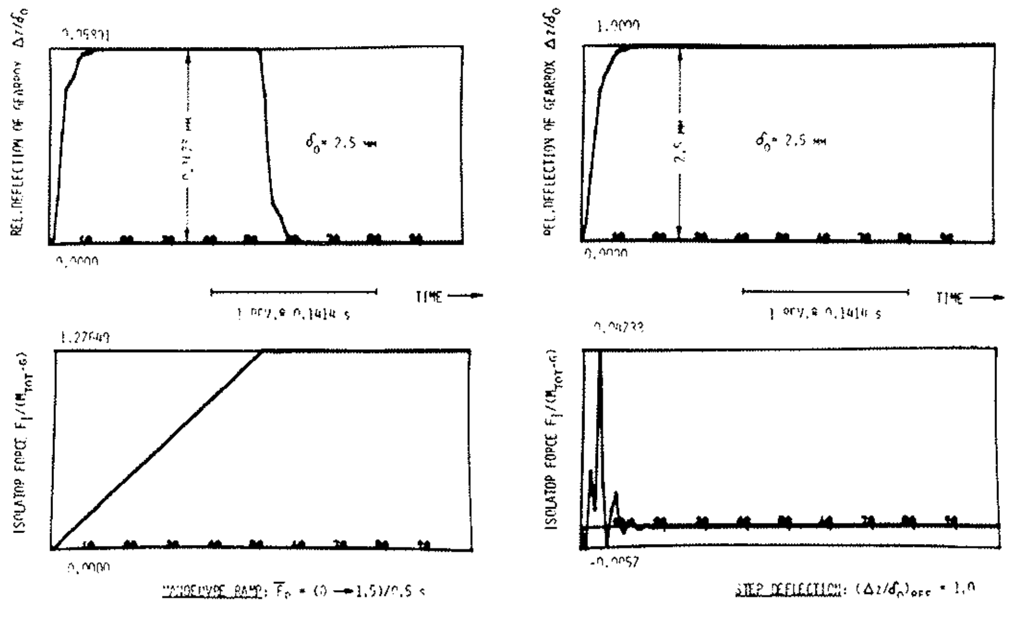

FIGURE 10: OPTIMAL CONTROLLER RESPONSE ON MANOEUVRE RAMP LOAD AND STEP DEFLECTION (VERTICAL AXIS, BO 105)

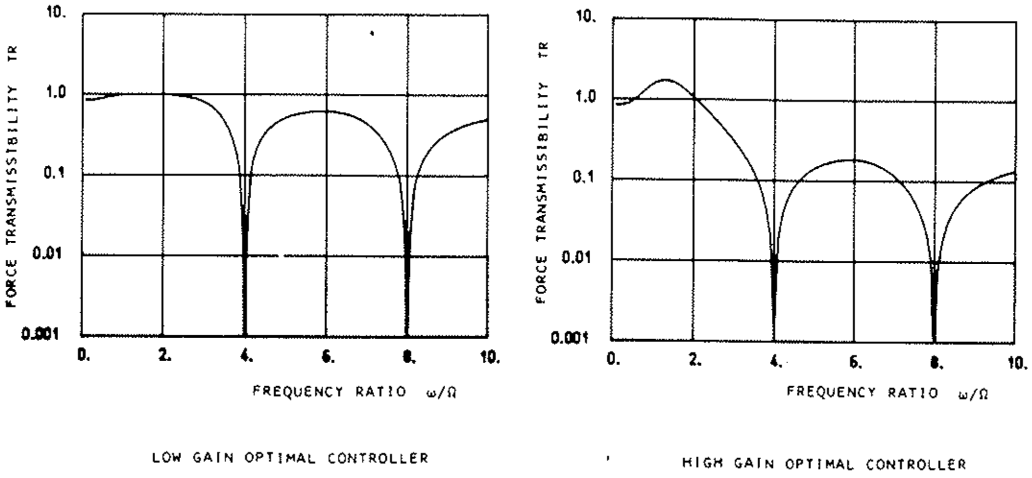

FIGURE 11: OPTIMAL CONTROLLER FOR A SINGLE AXIS, TWO-FREQUENCY ROTOR ISOLATION SYSTEM (BO 105)

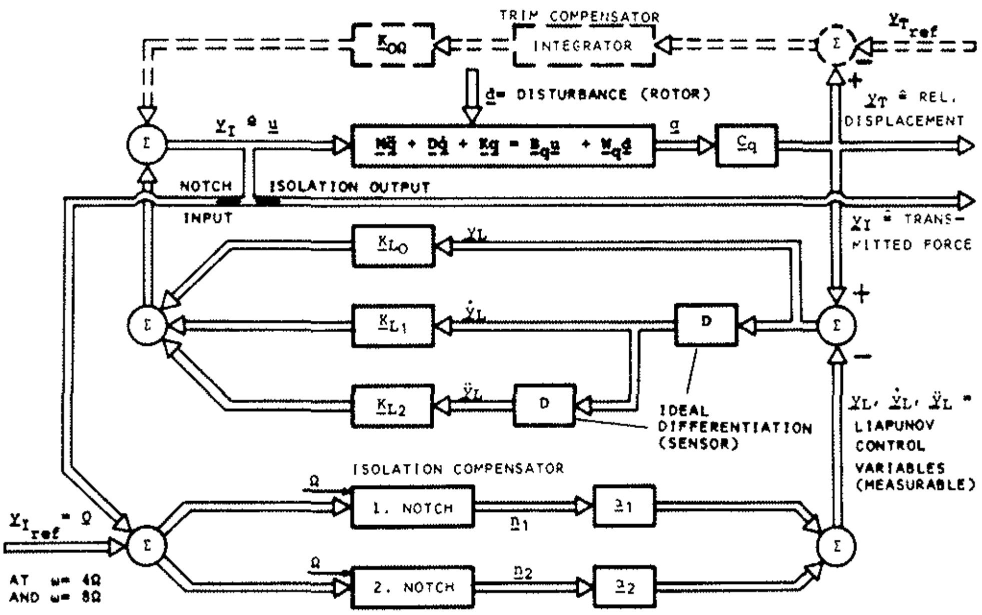

FIGURE 12: LIAPUNOV CONTROL CONFIGURATION FOR AN ACTIVE HELICOPTER ISOLATION SYSTEM (LAIER)

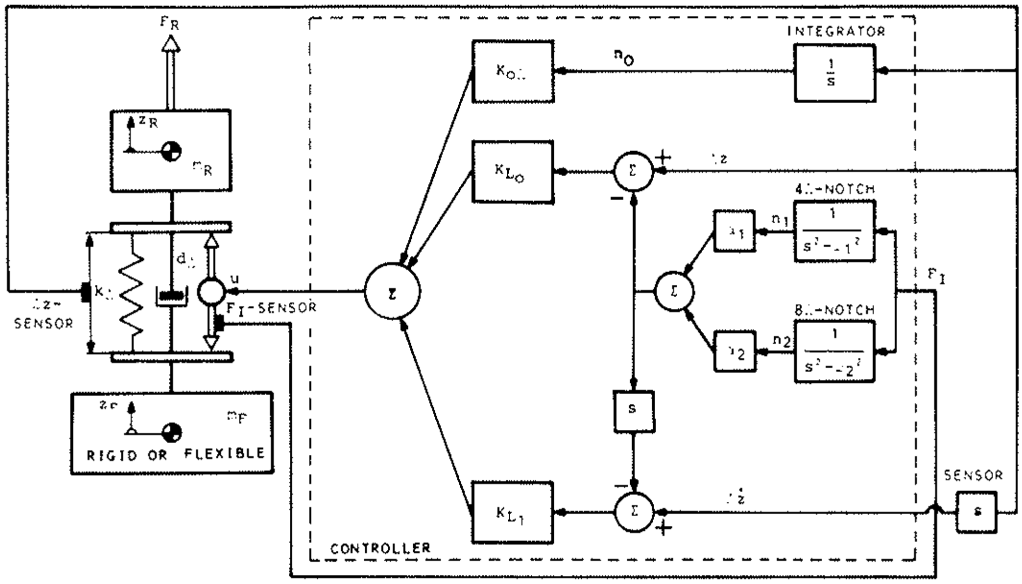

FIGURE 13: ACTIVE ISOLATION SYSTEM FOR THE VERTICAL AXIS
ENERGY CONTROLLER COMPLETED WITH INTEGRAL FEEDBACK

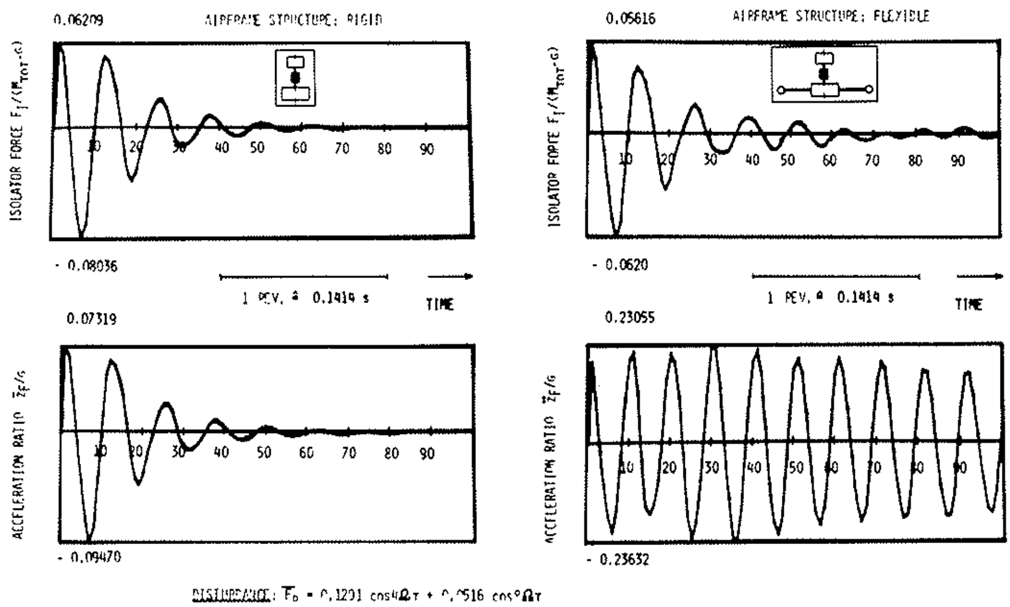

FIGURE 14: LIAPUNOV CONTROLLER RESPONSE ON HARMONIC DISTURBANCE
FOR RIGID AND FLEXIBLE MASS (VERTICAL AXIS, BO 105)

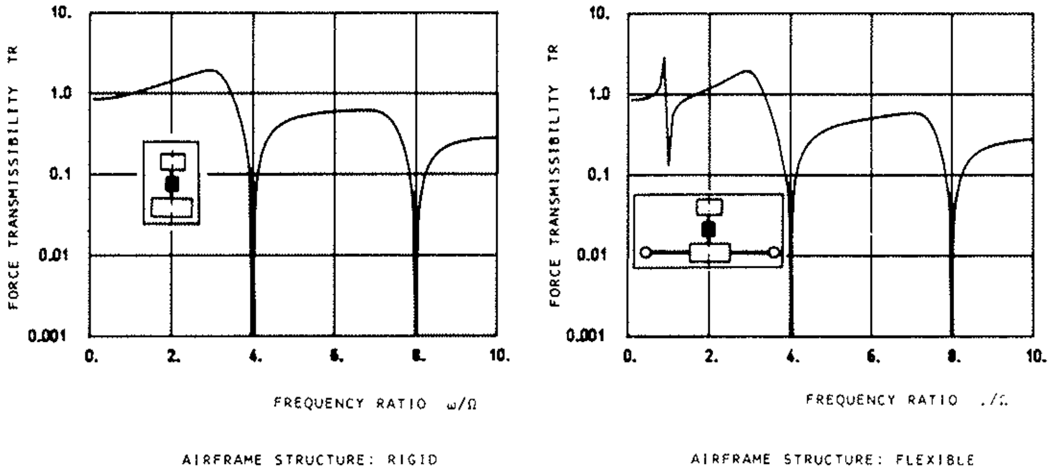

FIGURE 15: ENERGY CONTROLLER (LIAPUNOV) FOR A SINGLE AXIS ROTOR ISOLATION SYSTEM FOR RIGID AND FLEXIBLE MASS .

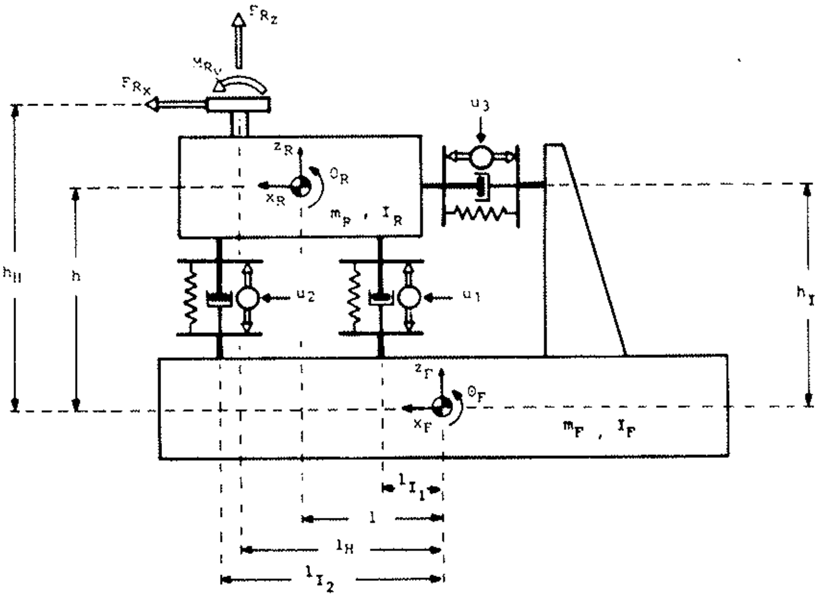

FIGURE 16: MODEL OF A MULTI-AXIS ROTOR ISOLATION SYSTEM

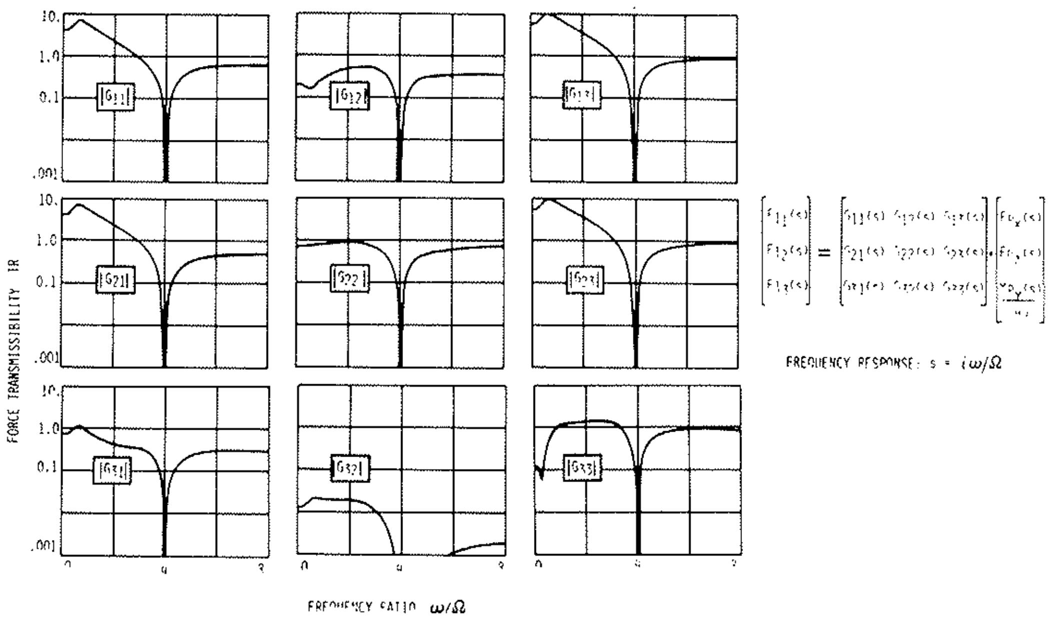

FIGURE 17: FORCE TRANSMISSIBILITY MATRIX FOR THE MULTI-AXIS ROTOR ISOLATION SYSTEM (BO 105)

ESTIMATED ISOLATION SYSTEM POWER REQUIREMENTS	
POWER REQUIRED FOR ISOLATION	2.7 kW
POWER REQUIRED FOR TRIM	1.8 kW
HYDRAULIC POWER (PUMP)	Σ: 4.5 kW
TOTAL POWER REQUIRED	5.6 kW

ROUGH ESTIMATES OF ISOLATION SYSTEM POWER, WEIGHT AND COST	
ISOLATION SYSTEM POWER (INSTALLED)	5.9 kW
% DRIVE POWER (INSTALLED)	1.1 %
ISOLATION SYSTEM WEIGHT	(24[1] ÷ 58) kg
% GROSS WEIGHT	(1.0[1] ÷ 2.4) %
ISOLATION SYSTEM COST	(93[1] ÷ 108) TDM
% VEHICLE COST	(9.3[1] ÷ 10.8) %

[1]: WITHOUT POWER PACKAGE

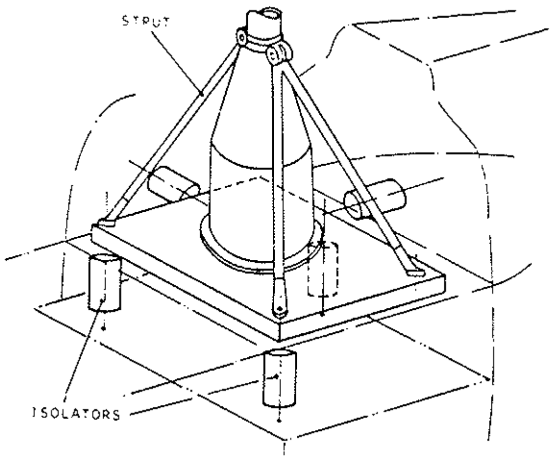

CONCEPT FOR MULTI-AXIS ISOLATION
(FIVE AXIS, FIVE ISOLATORS)

FIGURE 18: SUMMARY OF ESTIMATED POWER, WEIGHT AND COST OF AN ACTIVE ISOLATION SYSTEM FOR THE HELICOPTER BO 105

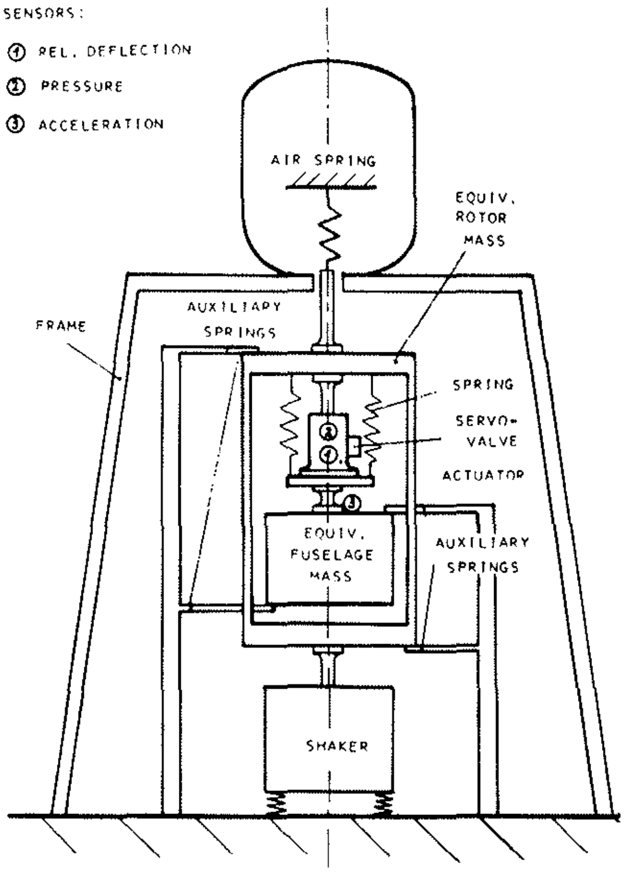

FIGURE 19: LABORATORY RESEARCH MODEL FOR ACTIVE ROTOR ISOLATION TESTS